

Bending-induced modulation doping: a promising tendency in silicon nanowires

Yuehan Li^{a}, Yue Zhang^{a*}, Suyang Zhang^a, Zun Xie^{†a} and Zhao Liu^{‡a}*

^aDepartment of Physics and Hebei Advanced Thin Film Laboratory, Hebei Normal University, Shijiazhuang, 050024, China

[†]Corresponding author: zxie@hebtu.edu.cn

[‡]Corresponding author: zliu@hebtu.edu.cn

* These authors contributed equally.

S1. Doping preference for [001]-oriented tetrahedral SiNW.

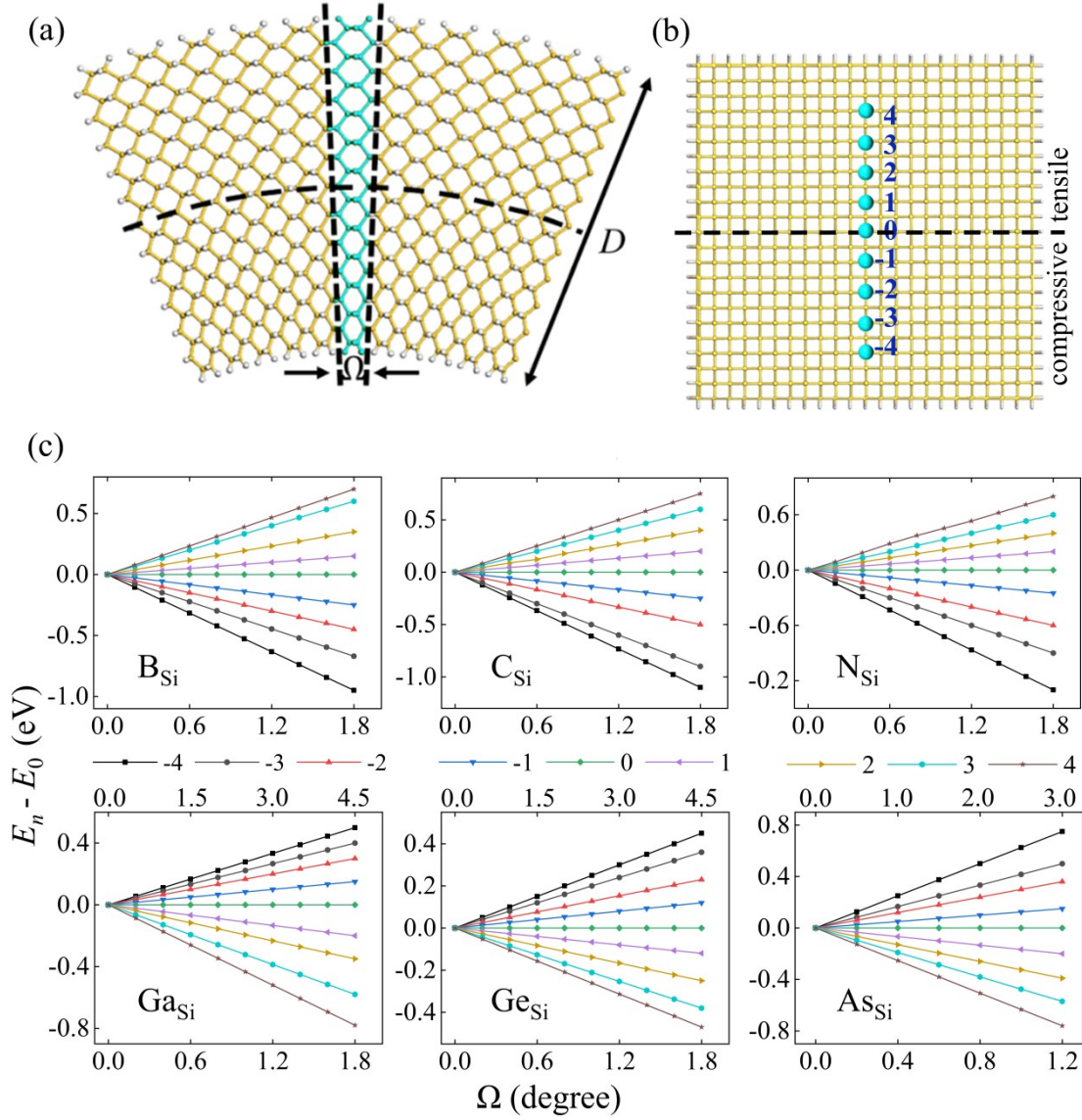


FIG. S1 (a) A side view of a bent tetrahedral SiNW along the [111] growth direction, with a diameter $D = 4.22$ nm. Ω represents the bending angle, and the dashed arc indicates the strain-free neutral surface. The primitive motif used in calculation is shown in green. (b) A cross-section of the SiNW depicted in (a), with 9 doping sites (red balls): sites $n = 1, 2, 3, 4$ are on the tensile side, sites $n = -1, -2, -3, -4$ are on the compressive side, site $n = 0$ is on the neutral surface. (c) The relative formation energy $E_n - E_0$ at site n versus

the bending angle Ω . X_{Si} ($X = \text{B}, \text{C}, \text{N}, \text{Ga}, \text{Ge}, \text{As}$) denotes the doping cases where the host Si atom is substituted with the dopant X atom.

S2. Energy bands and carrier distributions for [001]-oriented SiNW

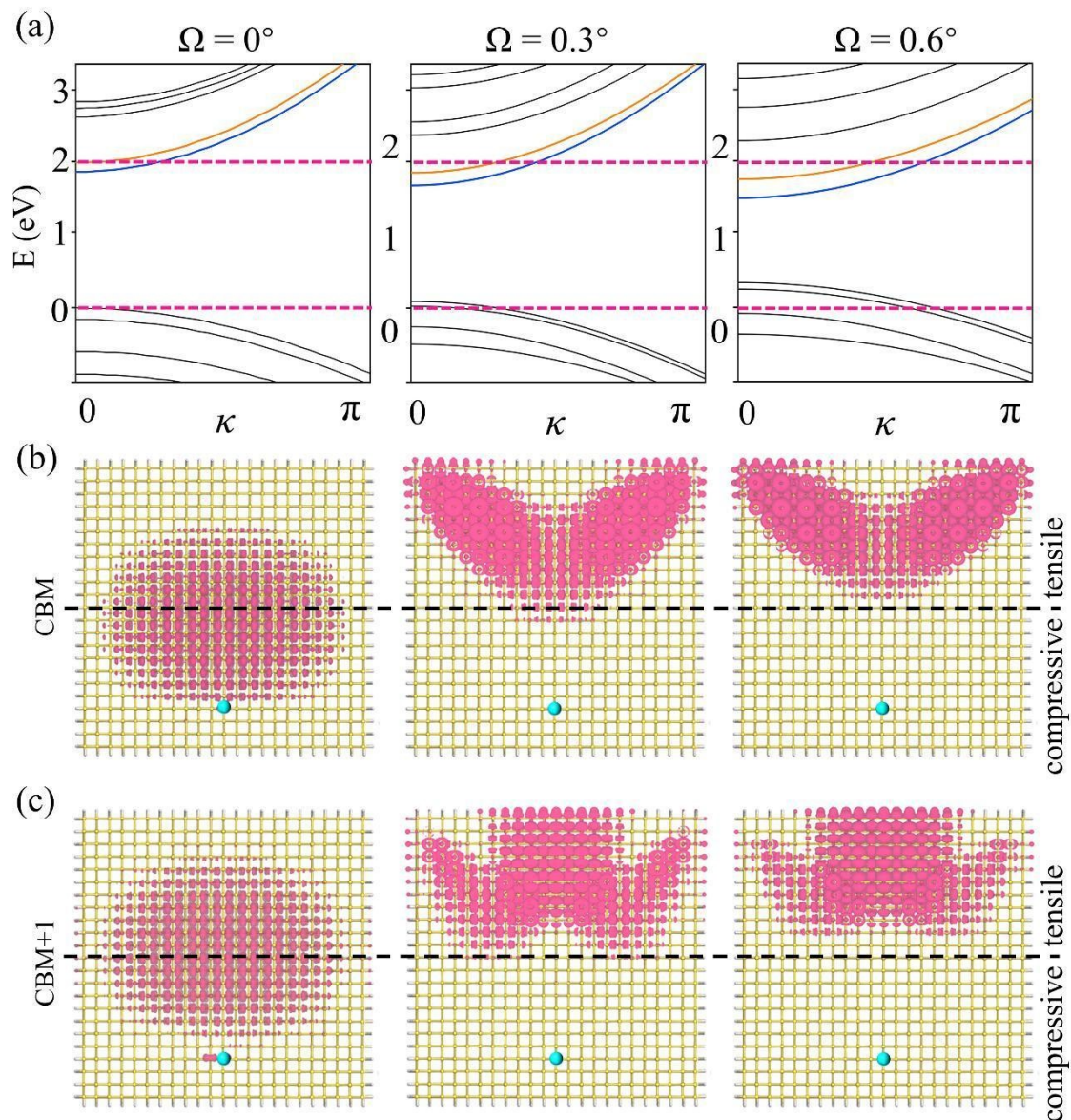


FIG. S2 [001]-oriented SiNW with a diameter of $D = 4.22$ nm after N doped at position $n = -4$. (a) Electronic energy bands for strain-free NW and bending angles with $\Omega = 0.3^\circ$ and $\Omega = 0.6^\circ$. Electronic density distribution (pink spheres) for the (b) CBM state and (c) the CBM+1 state, where the CBM state corresponds to the blue line in Fig. S2(a) and the CBM+1 state corresponds to the orange line in Fig. S2(a). Dopants are represented by blue spheres. The isosurface level is $1.72 \times 10^{-6} \text{ e } \text{\AA}^{-3}$.

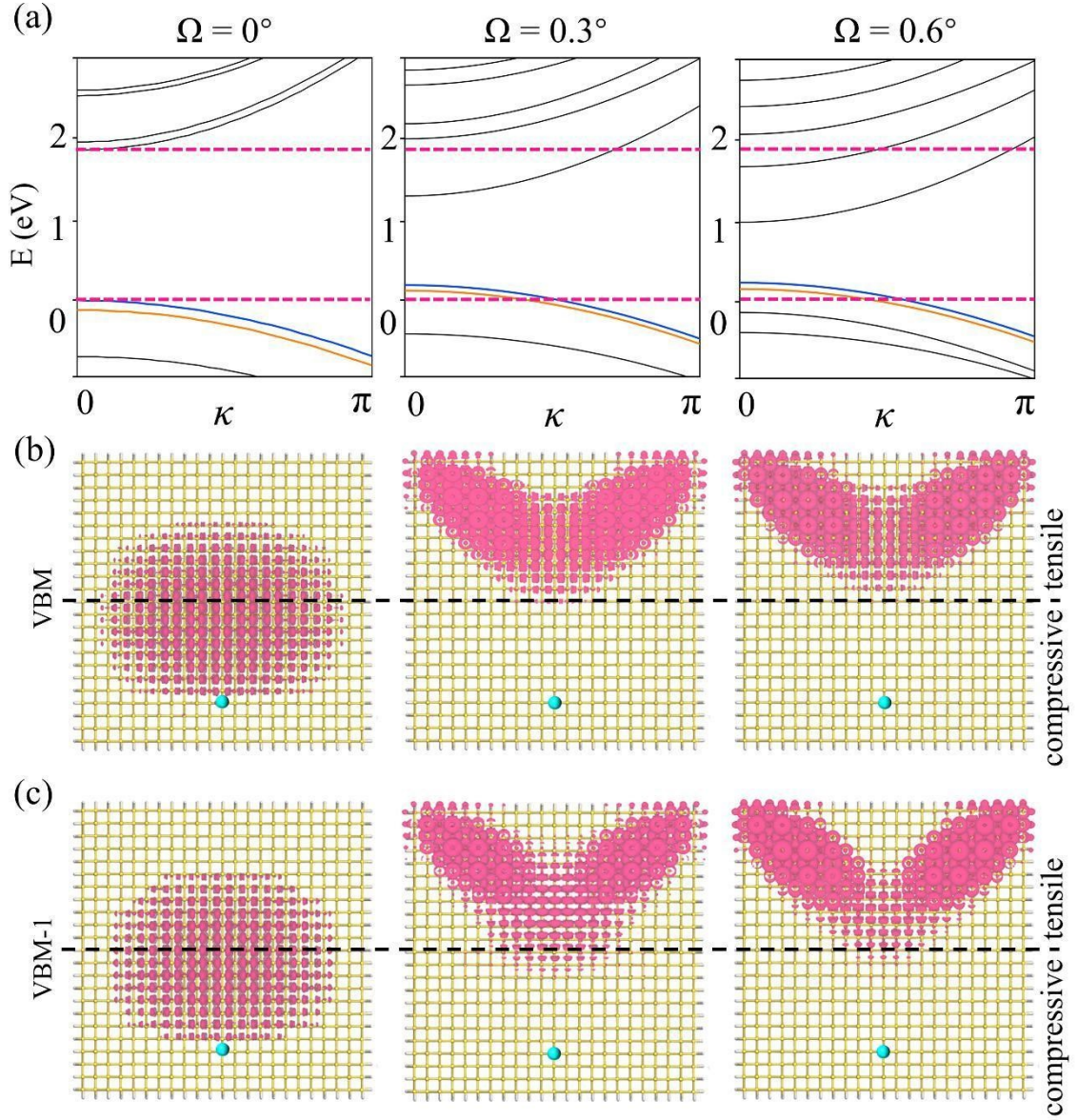


FIG. S3 [001]-oriented SiNW with a diameter of $D = 4.22$ nm after B doped at position $n = -4$. (a) Electronic energy bands for strain-free NW and bending angles with $\Omega = 0.3^\circ$ and $\Omega = 0.6^\circ$. Electronic density distribution (pink spheres) for the (b) VBM state and (c) the VBM-1 state, where the VBM state corresponds to the blue line in Fig. S3(a) and the VBM-1 state corresponds to the orange line in Fig. S3(a). Dopants are represented by blue spheres. The isosurface level is $1.72 \times 10^{-6} \text{ e \AA}^{-3}$.

S3. Band structure for bulk Si.

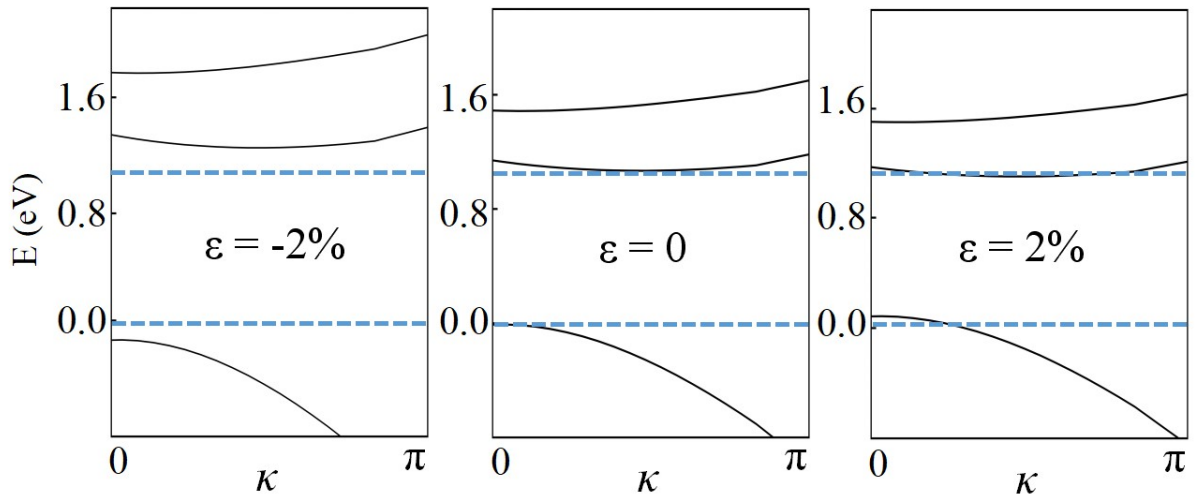


FIG. S4 Energy band of bulk Si with uniaxial tension and compression along the [001] direction of the SiNW.

S4. The comparison between DFTB+ and DFT data.

System	Method	Band gap (eV)
	DFTB+	1.31
	GGA	0.607 ⁽¹⁾
bulk Si	BLYP	1.39 ⁽²⁾
	BPBE	1.13 ⁽²⁾
	Exp.	~1.17 ⁽³⁾

Table S1 The calculated band gaps with different methods of bulk silicon.

System	Diameter (nm)	Band gap (eV)	Ref. Band gap (eV)
	0.92	2.85	2.25 ⁽⁴⁾
[111] Si NW	1.69	2.21	1.34 ⁽⁴⁾
	2.46	2.04	1.13 ⁽⁴⁾
	1.2	2.14	1.51 ⁽⁴⁾
[011] Si NW	2.2	1.77	0.89 ⁽⁴⁾
	3.3	1.55	0.78 ⁽⁴⁾
[001] Si NW	1.1	3.23	2.35 ⁽⁵⁾
	2.0	2.58	1.32 ⁽⁵⁾

Table S2 The calculated band gaps comparison of SiNWs along different orient.

⁽¹⁾Crystals **14**, 585 (2024).

⁽²⁾Phys. Rev. B **76**, 155435 (2007).

⁽³⁾ Solid State Phys. **1**, 2 (1976).

⁽⁴⁾Phys. Rev. B **74**, 045116 (2006).

⁽⁵⁾Phys. Rev. Lett. **92**, 236805 (2004).

S5. Calculations with supercell.

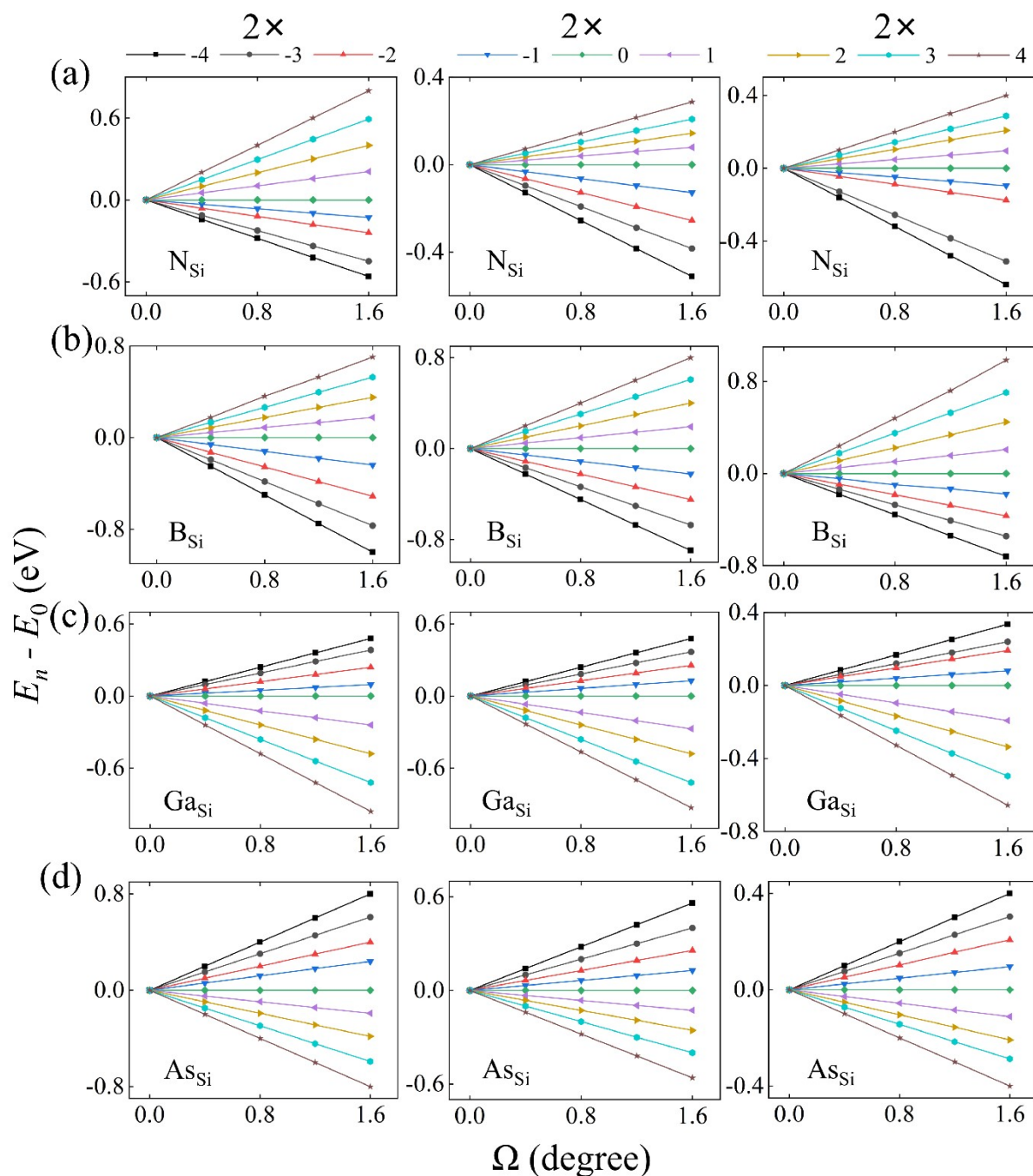


FIG. S5 The relative formation energy versus bending angle for [111]-oriented SiNWs with $D = 4.43$ nm in expanded supercells with doping at sites $n = -4, -3, -2, -1, 0, 1, 2, 3, 4$. The first, second, and third columns correspond to $2\times$, $3\times$, and $4\times$ supercells, respectively, with (a) N doping, (b) B doping, (c) Ga doping, and (d) As doping.

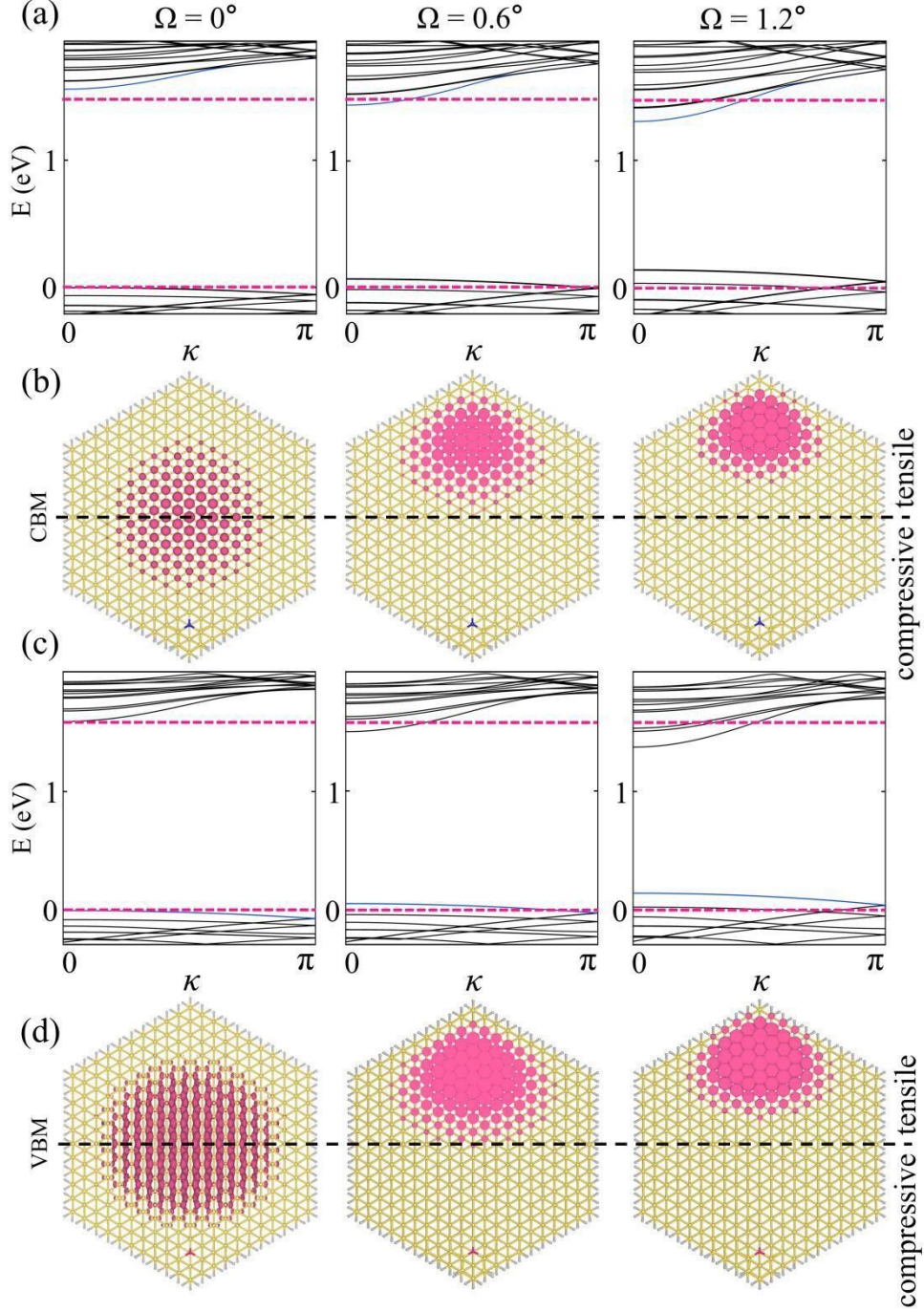


FIG. S6 [111]-oriented SiNW with a $2\times$ expanded supercell and a diameter of $D = 4.43$ nm after (a) (b) N and (c) (d) B doped at position $n = -4$. (a) (c) Electronic energy bands for strain-free NW and bending angles with $\Omega = 0.6^\circ$ and $\Omega = 1.2^\circ$. Electronic density distribution (pink spheres) for the (b) CBM state and (d) the VBM state. The isosurface level is $1.72 \times 10^{-6} e \text{ \AA}^{-3}$.

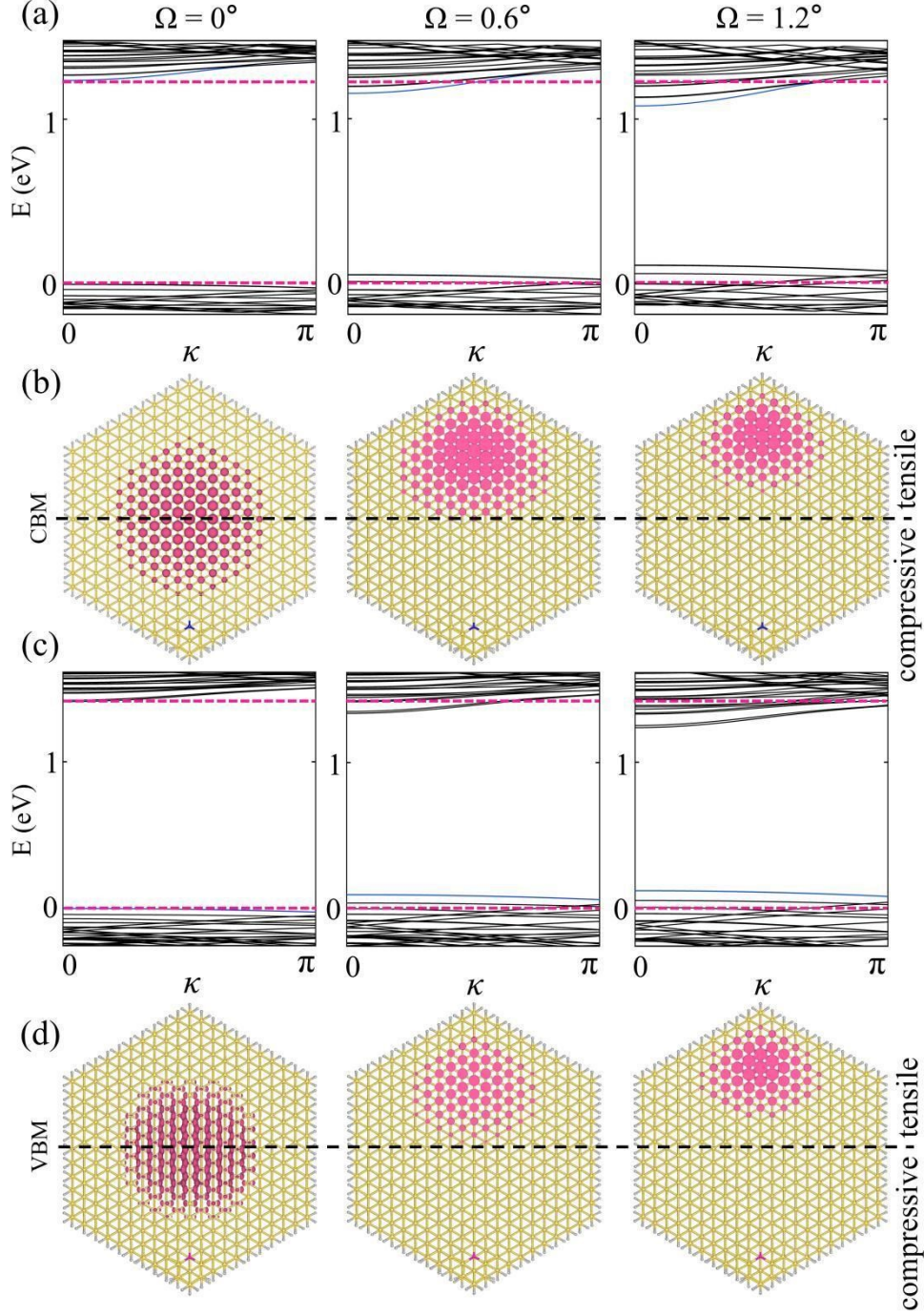


FIG. S7 [111]-oriented SiNW with a $3\times$ expanded supercell and a diameter of $D = 4.43$ nm after (a) (b) N and (c) (d) B doped at position $n = -4$. (a) (c) Electronic energy bands for strain-free NW and bending angles with $\Omega = 0.6^\circ$ and $\Omega = 1.2^\circ$. Electronic density distribution (pink spheres) for the (b) CBM state and (d) the VBM state. The isosurface level is $1.72 \times 10^{-6} e \text{ \AA}^{-3}$.

3.

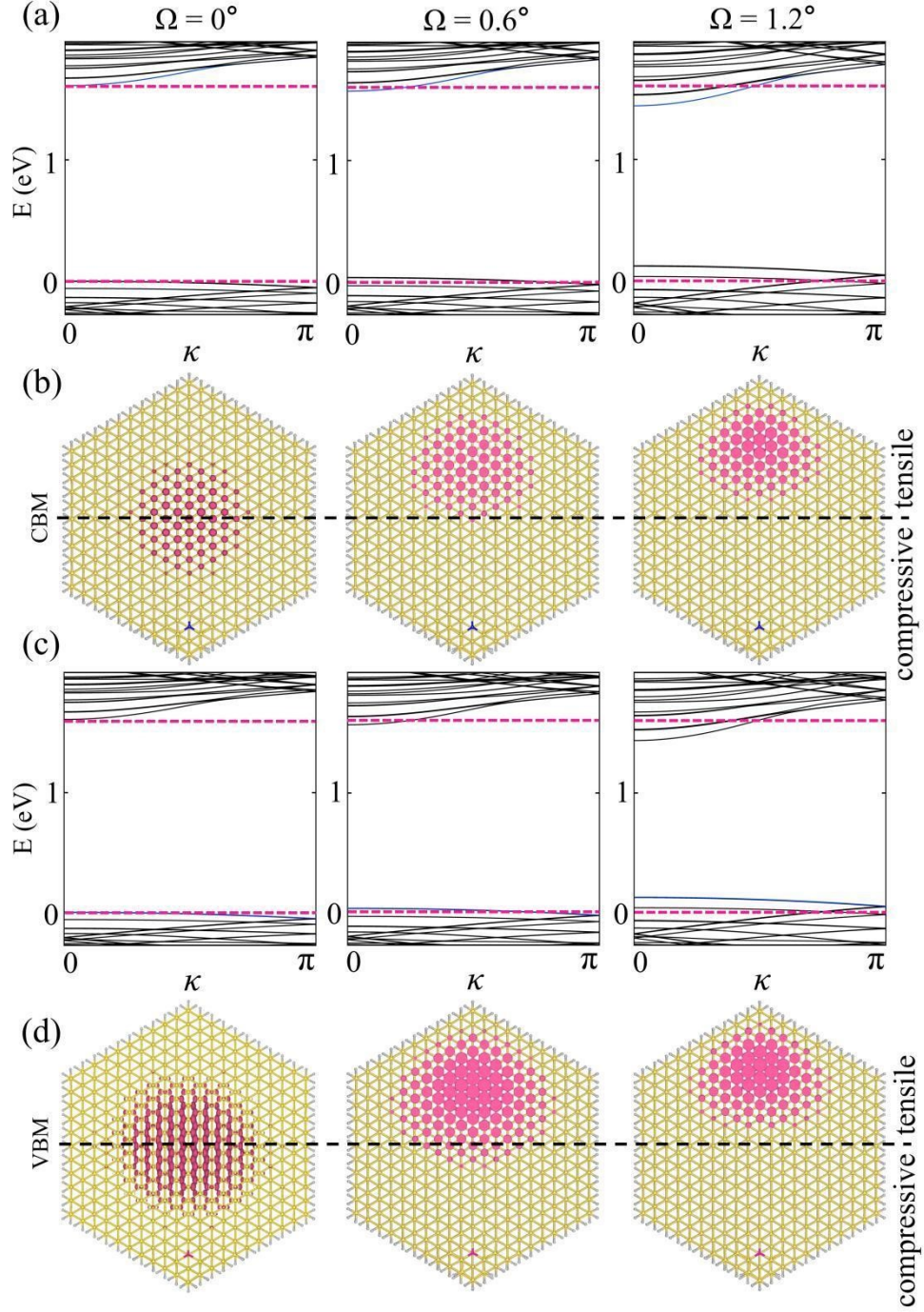


FIG. S8 [111]-oriented SiNW with a $4\times$ expanded supercell and a diameter of $D = 4.43$ nm after (a) (b) N and (c) (d) B doped at position $n = -4$. (a) (c) Electronic energy bands for strain-free NW and bending angles with $\Omega = 0.6^\circ$ and $\Omega = 1.2^\circ$. Electronic density distribution (pink spheres) for the (b) CBM state and (d) the VBM state. The isosurface level is $1.72 \times 10^{-6} e \text{ \AA}^{-3}$.

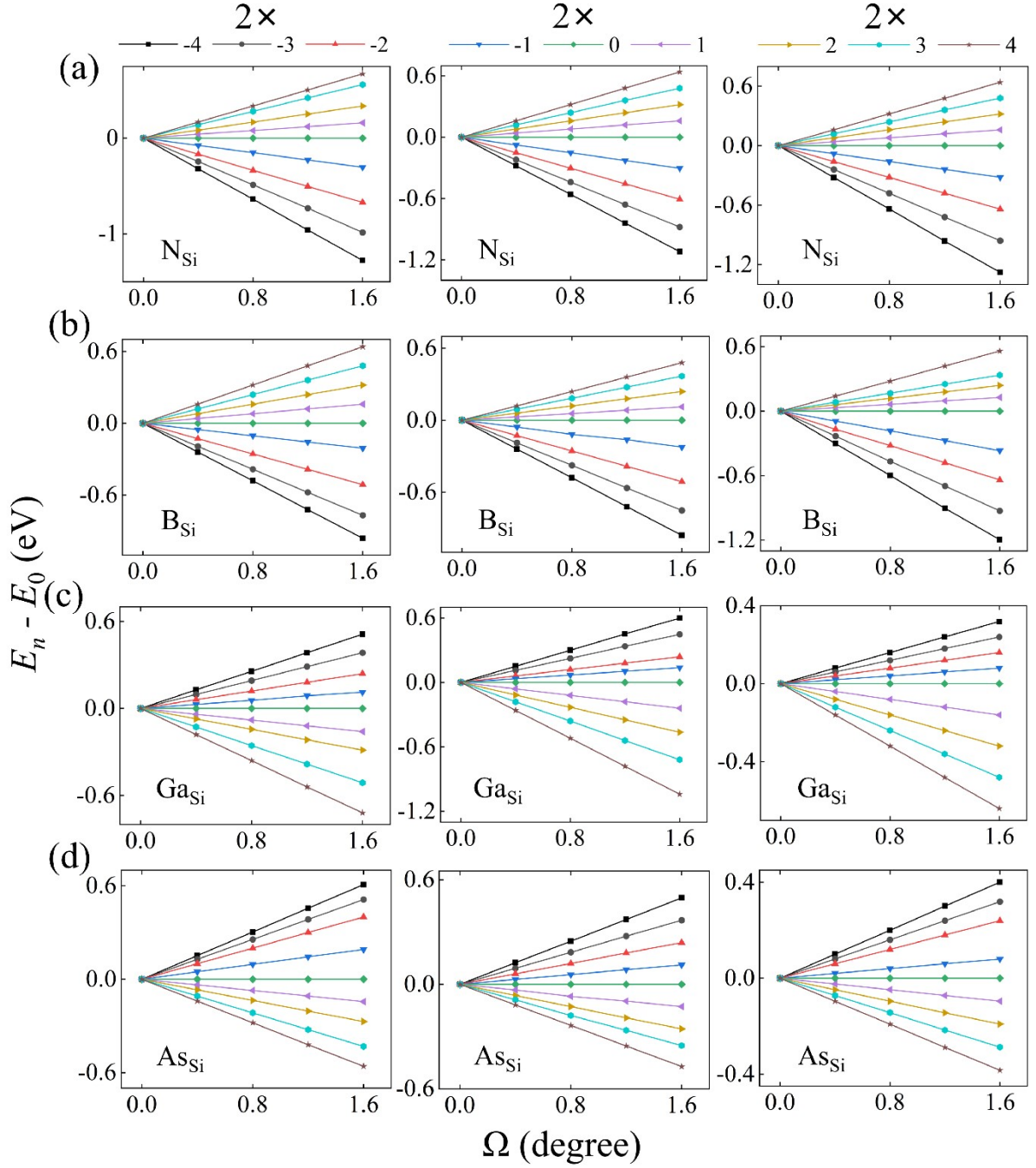


FIG. S9 The relative formation energy versus bending angle for [001]-oriented SiNWs with $D = 4.22$ nm in expanded supercells with doping at sites sites $n = -4, -3, -2, -1, 0, 1, 2, 3, 4$. The first, second, and third columns correspond to $2\times$, $3\times$, and $4\times$ supercells, respectively, with (a) N doping, (b) B doping, (c) Ga doping, and (d) As doping.

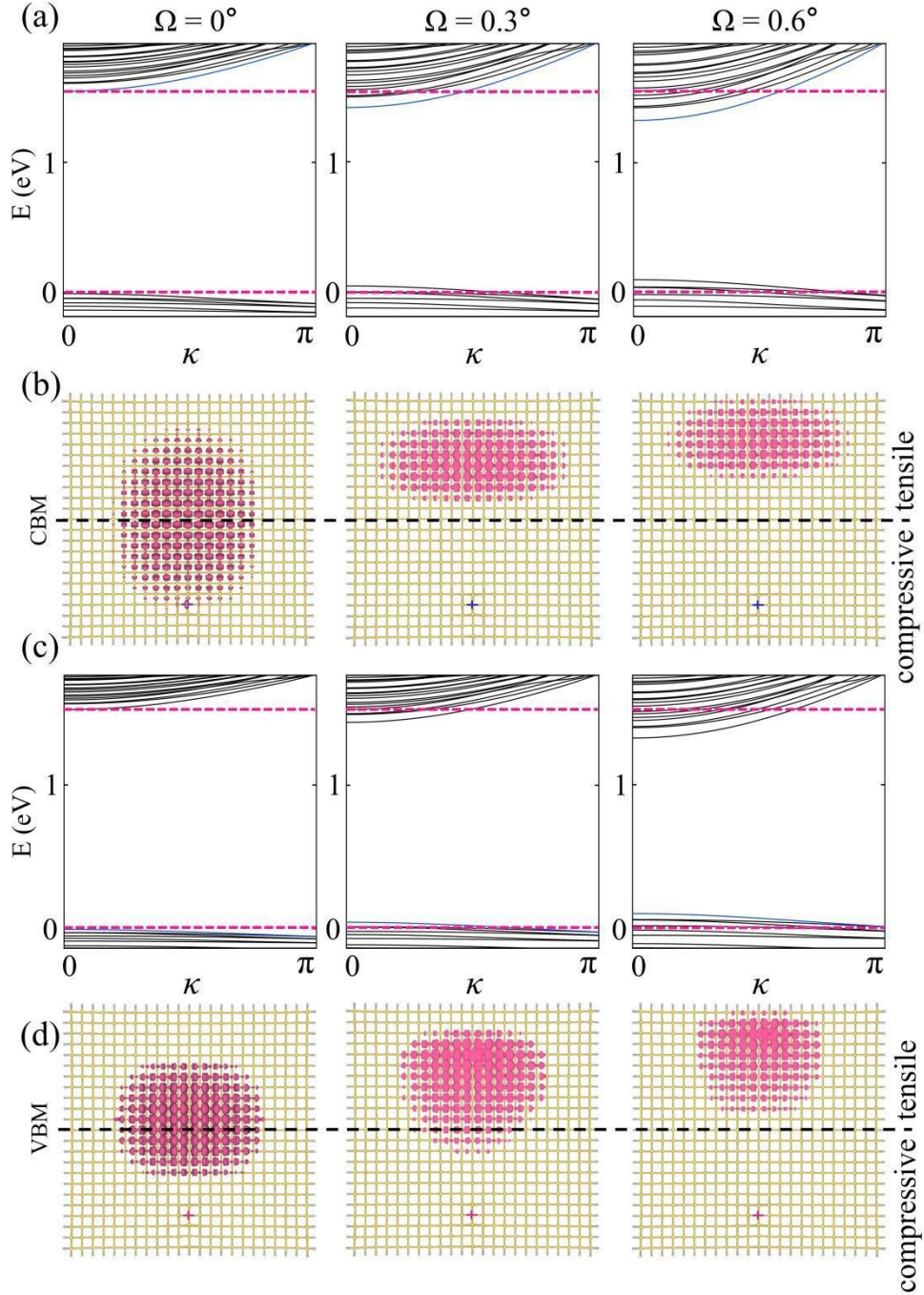


FIG. S10 [001]-oriented SiNW with a $2\times$ expanded supercell and a diameter of $D = 4.22$ nm after (a) (b) N and (c) (d) B doped at position $n = -4$. (a) (c) Electronic energy bands for strain-free NW and bending angles with $\Omega = 0.3^\circ$ and $\Omega = 0.6^\circ$. Electronic density distribution (pink spheres) for the (b) CBM state and (d) the VBM state. The isosurface level is $1.72 \times 10^{-6} e \text{ \AA}^{-3}$.

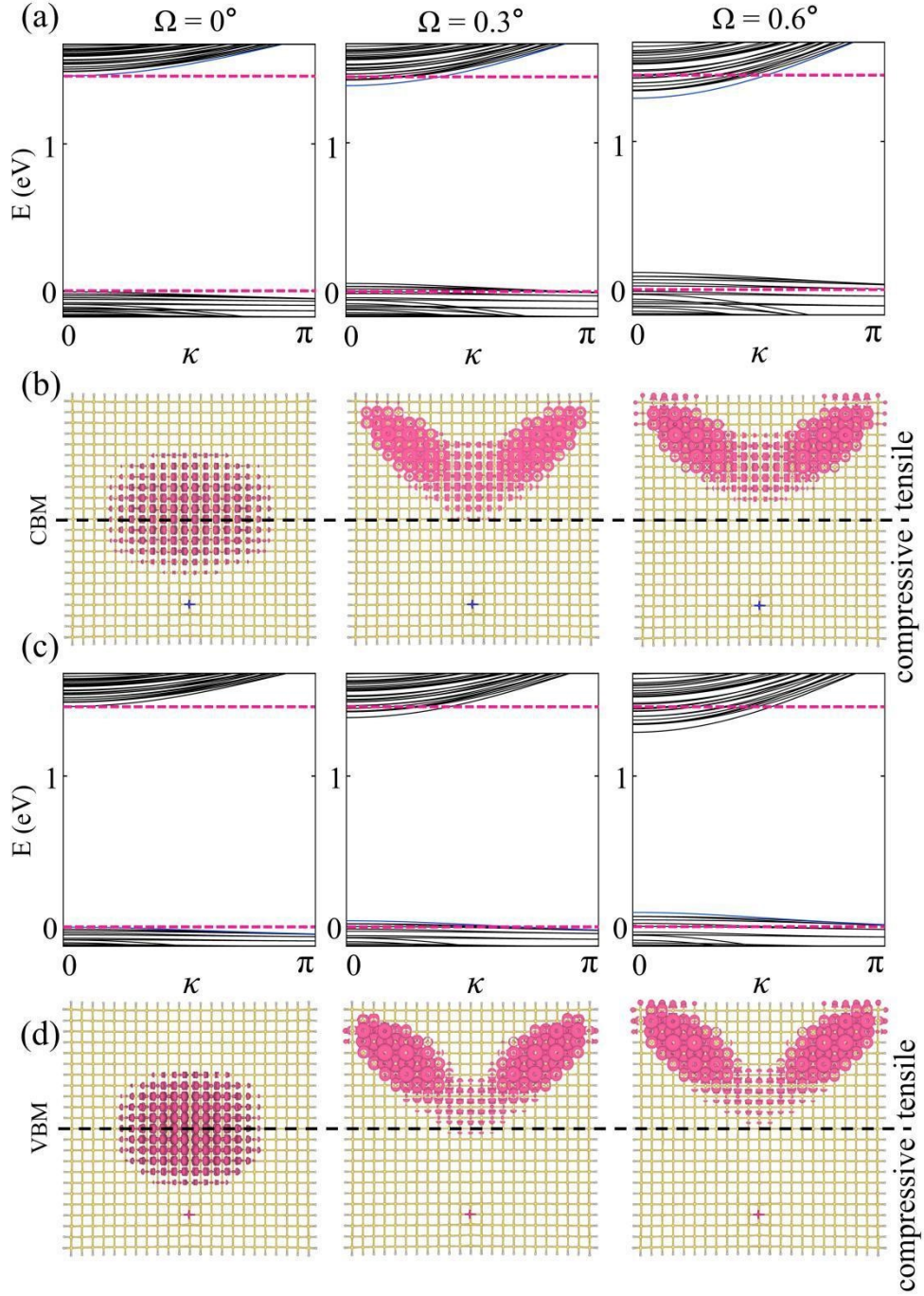


FIG. S11 [001]-oriented SiNW with a $3\times$ expanded supercell and a diameter of $D = 4.22$ nm after (a) (b) N and (c) (d) B doped at position $n = -4$. (a) (c) Electronic energy bands for strain-free NW and bending angles with $\Omega = 0.3^\circ$ and $\Omega = 0.6^\circ$. Electronic density distribution (pink spheres) for the (b) CBM state and (d) the VBM state. The isosurface level is $1.72 \times 10^{-6} e \text{ \AA}^{-3}$.

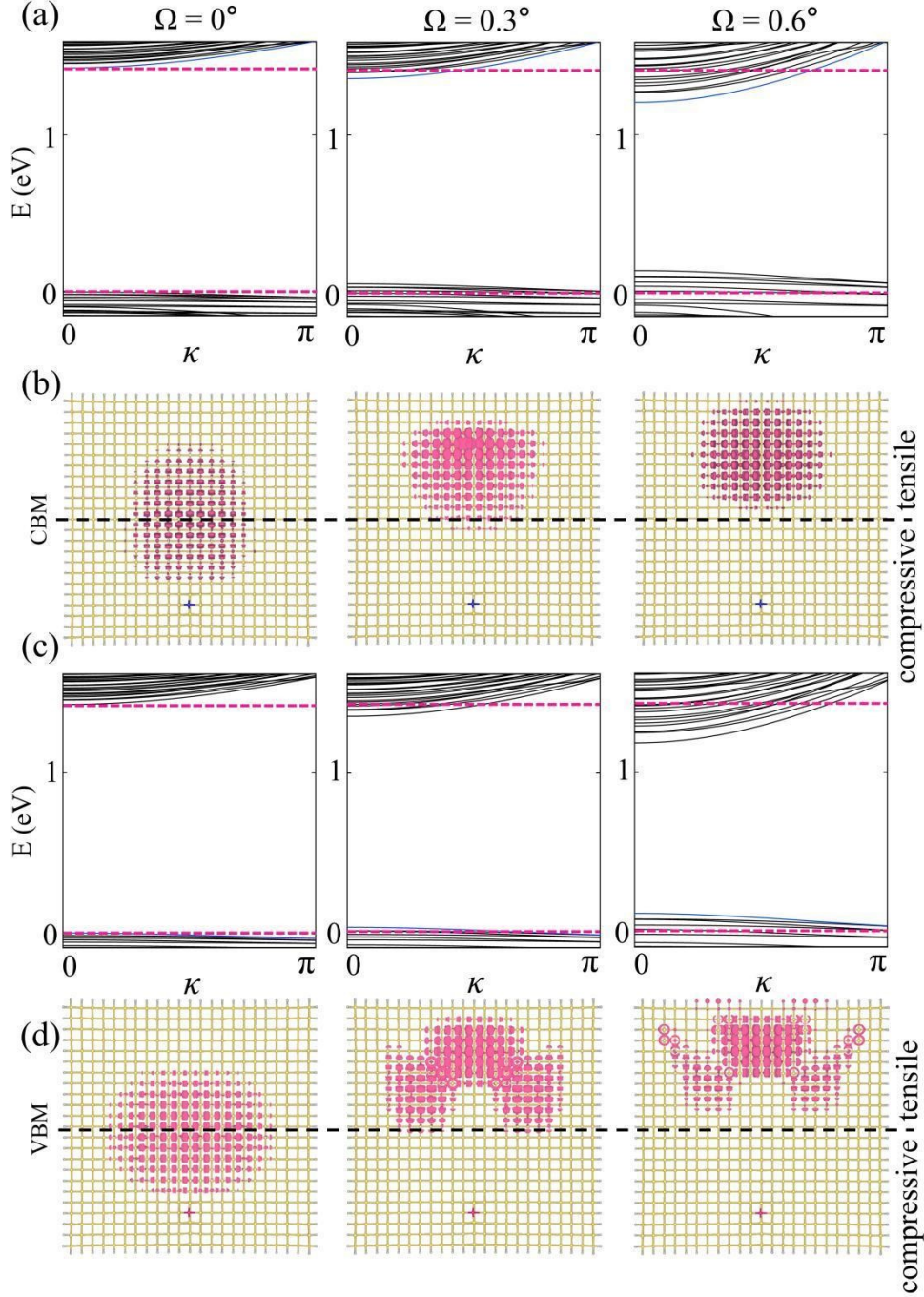


FIG. S12 [001]-oriented SiNW with a $4\times$ expanded supercell and a diameter of $D = 4.22$ nm after (a) (b) N and (c) (d) B doped at position $n = -4$. (a) (c) Electronic energy bands for strain-free NW and bending angles with $\Omega = 0.3^\circ$ and $\Omega = 0.6^\circ$. Electronic density distribution (pink spheres) for the (b) CBM state and (d) the VBM state. The isosurface level is $1.72 \times 10^{-6} e \text{ \AA}^{-3}$.

S5. Calculations with different diameters.

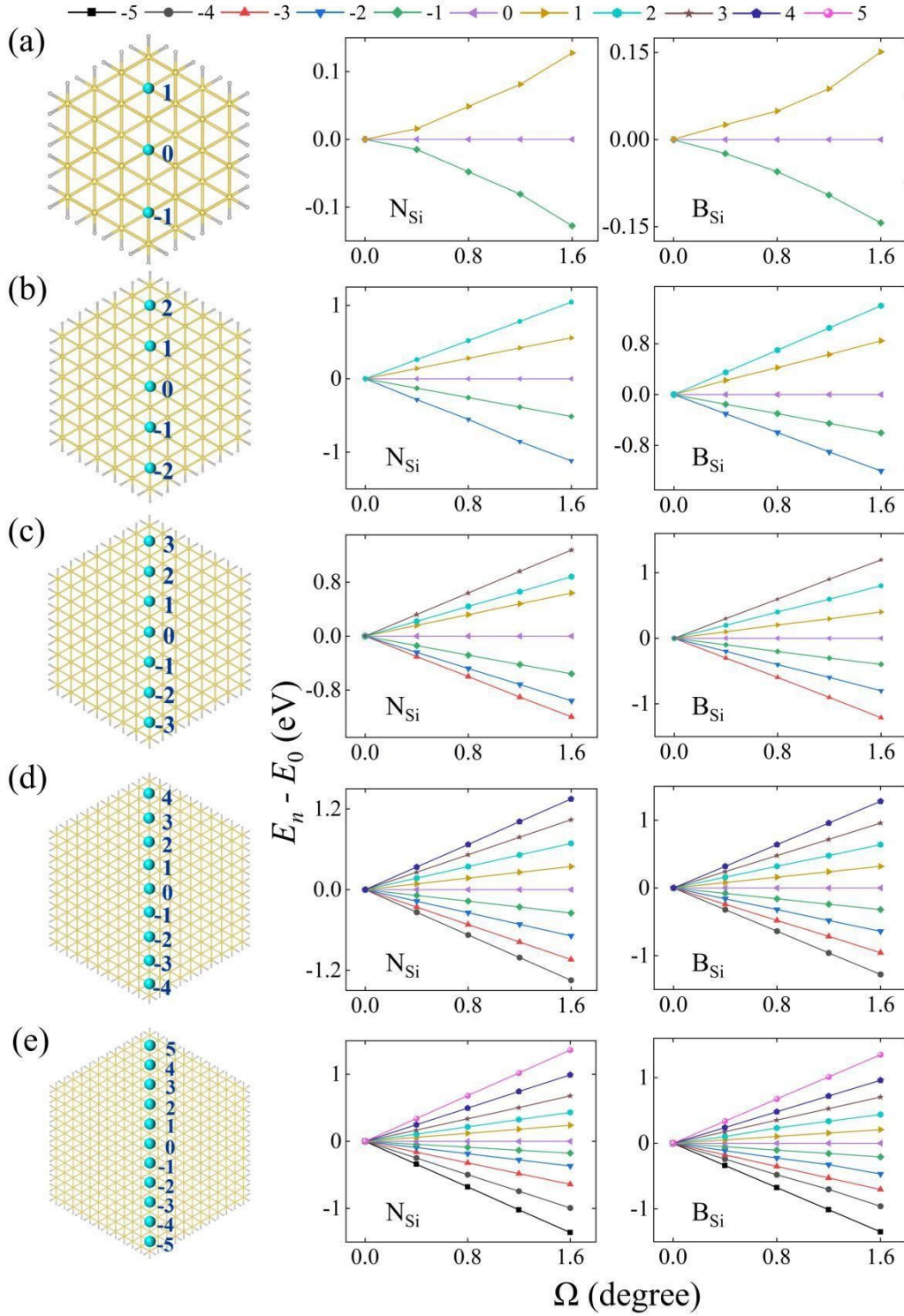


FIG. S13 [111]-oriented SiNW with a diameter of $D =$ (a) 1.32 nm, (b) 2.24 nm, (c) 3.1 nm, (d) 3.99 nm, (e) 4.89 nm, with 11 doping sites (blue balls): sites $n = 1, 2, 3, 4, 5$ are on the tensile side, sites $n = -1, -2, -3, -4, -5$ are on the compressive side, and site $n = 0$ is on the neutral

surface. The last two columns are The relative formation energy $E_n - E_0$ at site n versus bending angle Ω for various doping cases, denoted as X_{Si} ($X = \text{B}, \text{N}$), where the host Si atom is substituted with the dopant X atom.

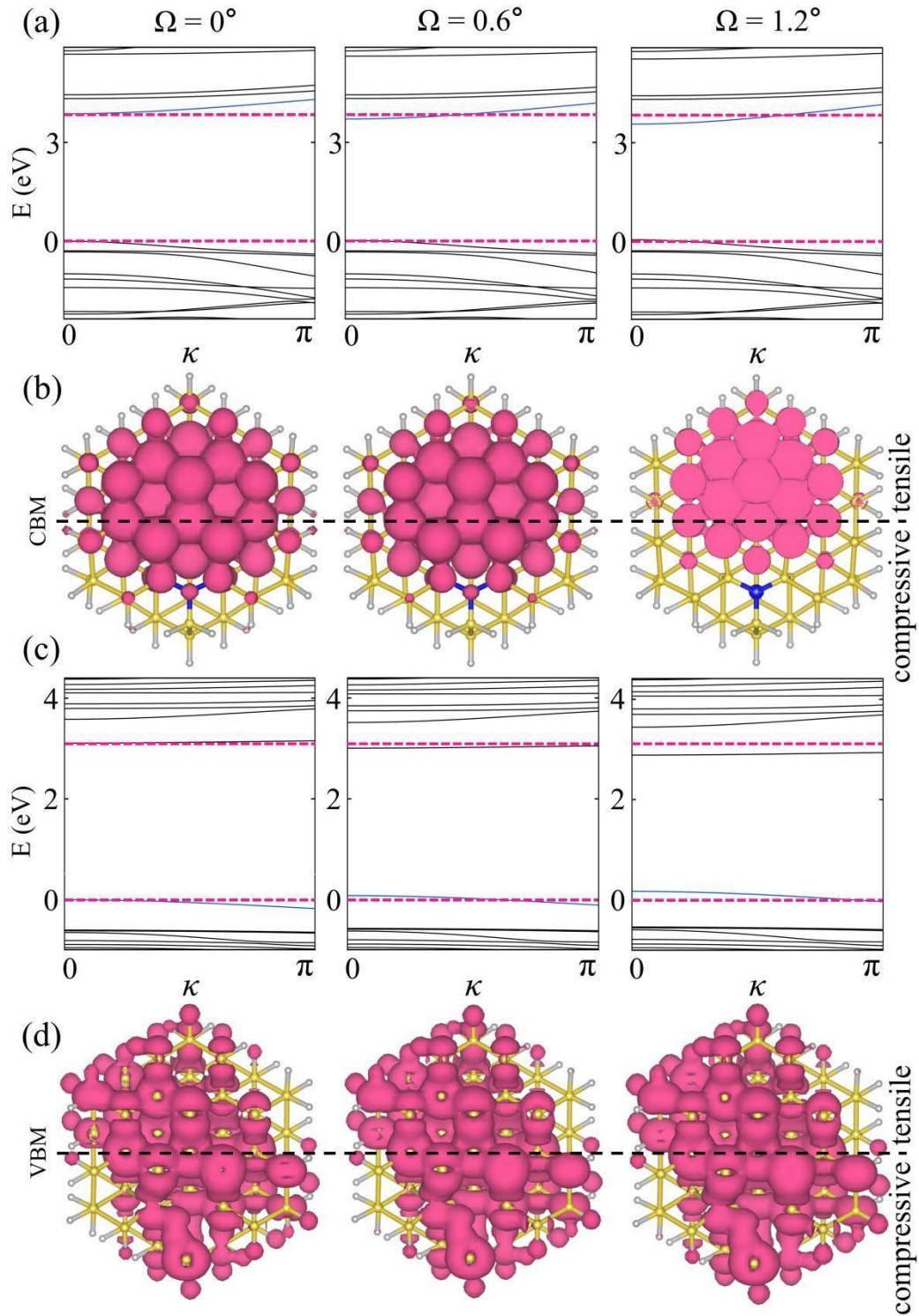


FIG. S14 [111]-oriented SiNW with a diameter of $D = 1.32$ nm after (a) (b) N and (c) (d) B doped at position $n = -4$. (a) (c) Electronic energy bands for strain-free NW and bending angles with $\Omega = 0.6^\circ$ and $\Omega = 1.2^\circ$. Electronic density distribution (pink spheres) for the (b) CBM state and (d) the VBM state. The isosurface level is $1.72 \times 10^{-6} e \text{ \AA}^{-3}$.

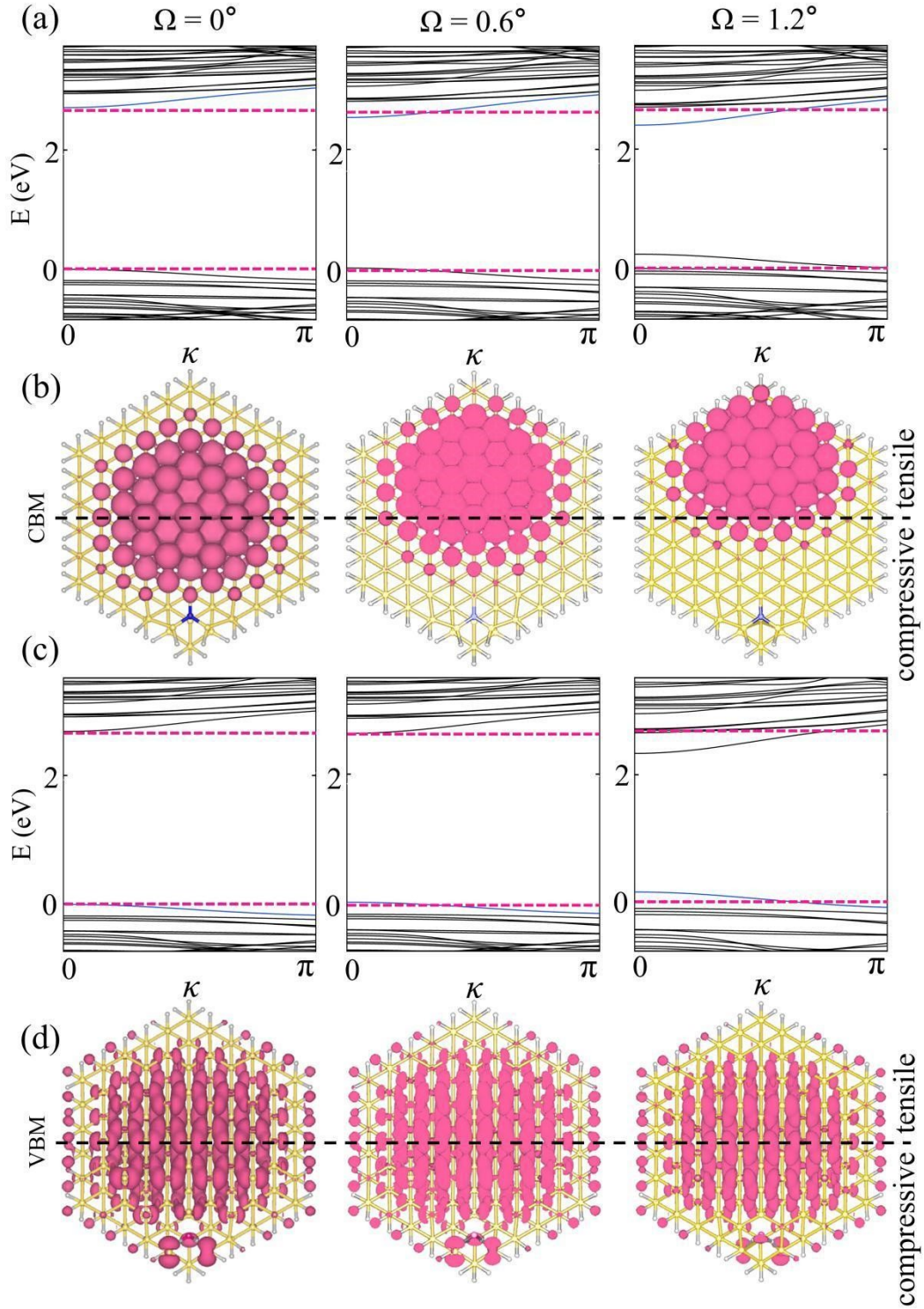


FIG. S15 [111]-oriented SiNW with a diameter of $D = 2.24$ nm after (a) (b) N and (c) (d) B doped at position $n = -4$. (a) (c) Electronic energy bands for strain-free NW and bending angles with $\Omega = 0.6^\circ$ and $\Omega = 1.2^\circ$. Electronic density distribution (pink spheres) for the (b) CBM state and (d) the VBM state. The isosurface level is $1.72 \times 10^{-6} e \text{ \AA}^{-3}$.

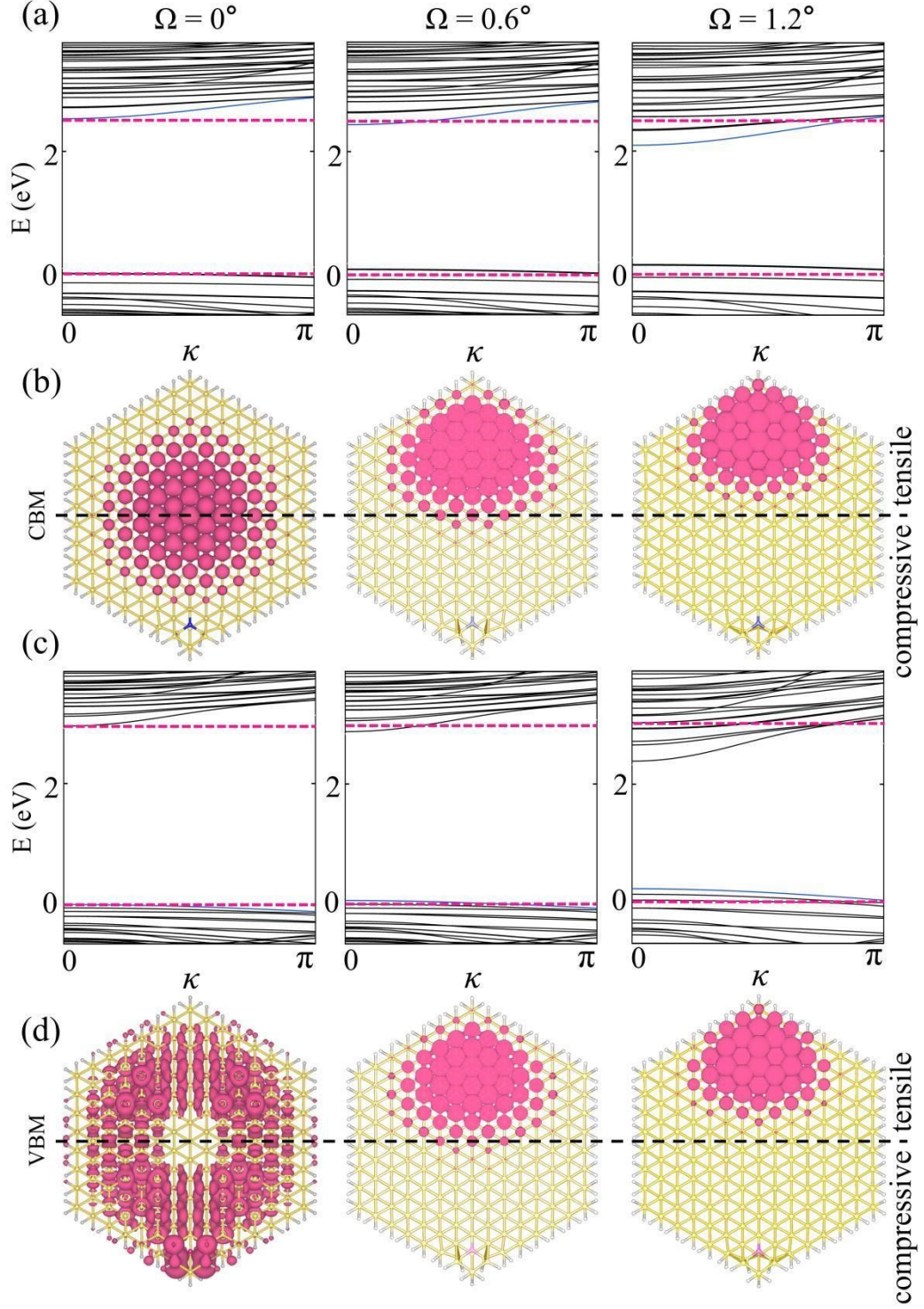


FIG. S16 [111]-oriented SiNW with a diameter of $D = 3.1$ nm after (a) (b) N and (c) (d) B doped at position $n = -4$. (a) (c) Electronic energy bands for strain-free NW and bending angles with $\Omega = 0.6^\circ$ and $\Omega = 1.2^\circ$. Electronic density distribution (pink spheres) for the (b) CBM state and (d) the VBM state. The isosurface level is $1.72 \times 10^{-6} e \text{ \AA}^{-3}$.

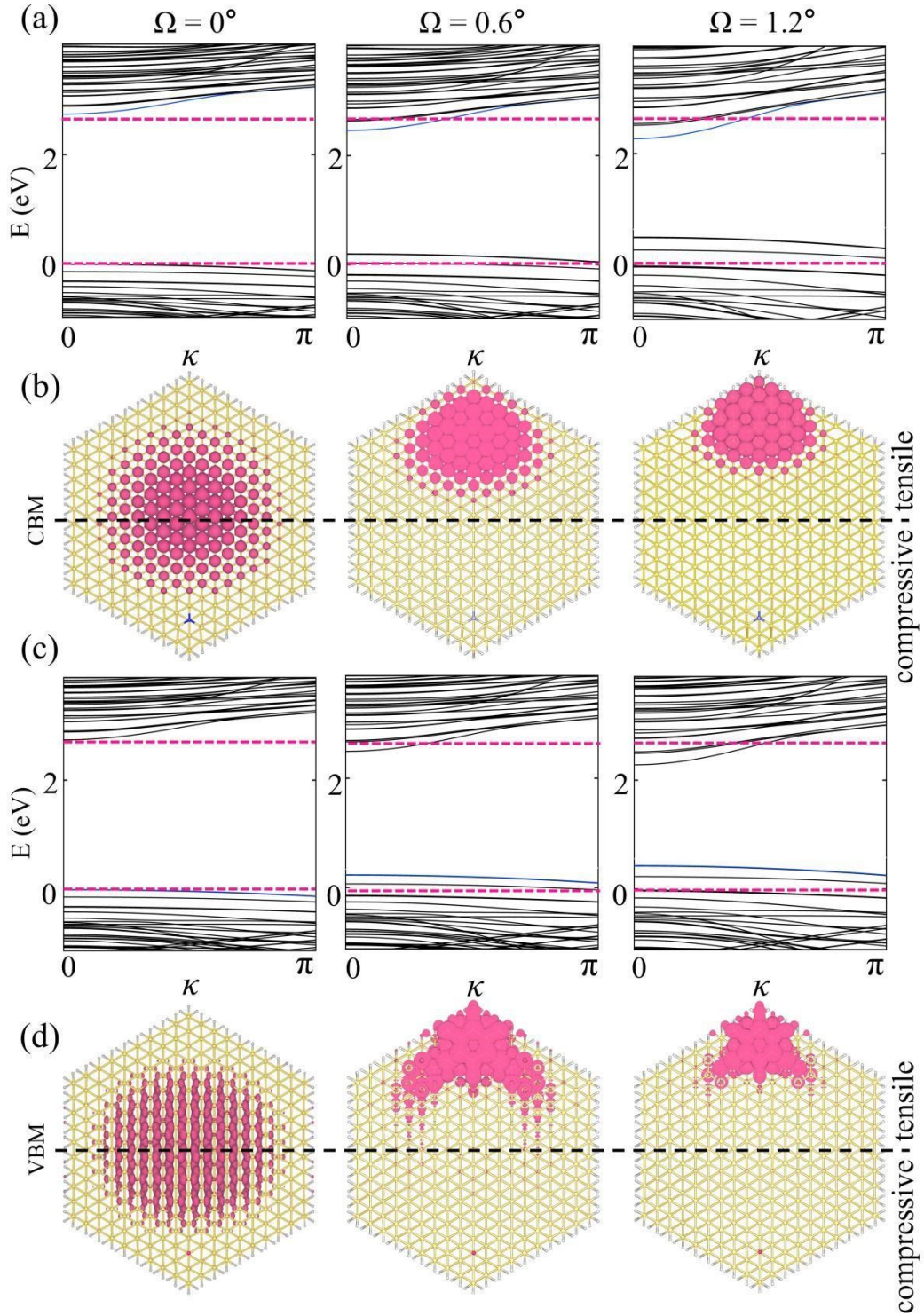


FIG. S17 [111]-oriented SiNW with a diameter of $D = 3.99$ nm after (a) (b) N and (c) (d) B doped at position $n = -4$. (a) (c) Electronic energy bands for strain-free NW and bending angles

with $\Omega = 0.6^\circ$ and $\Omega = 1.2^\circ$. Electronic density distribution (pink spheres) for the (b) CBM state and (d) the VBM state. The isosurface level is $1.72 \times 10^{-6} \text{ e \AA}^{-3}$.

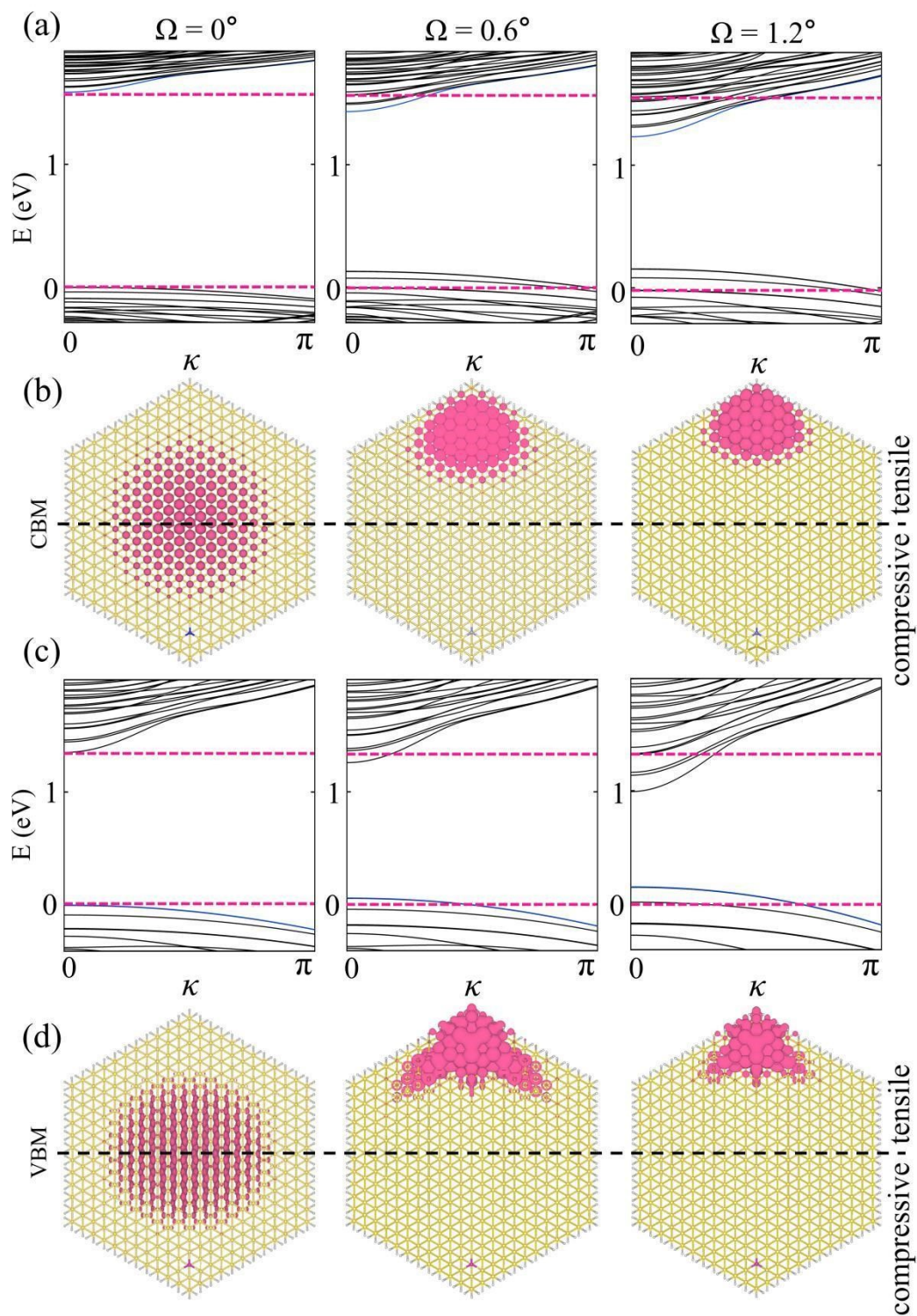


FIG. S18 [111]-oriented SiNW with a diameter of $D = 4.89 \text{ nm}$ after (a) (b) N and (c) (d) B doped at position $n = -4$. (a) (c) Electronic energy bands for strain-free NW and bending angles

with $\Omega = 0.6^\circ$ and $\Omega = 1.2^\circ$. Electronic density distribution (pink spheres) for the (b) CBM state and (d) the VBM state. The isosurface level is $1.72 \times 10^{-6} e \text{ \AA}^{-3}$.

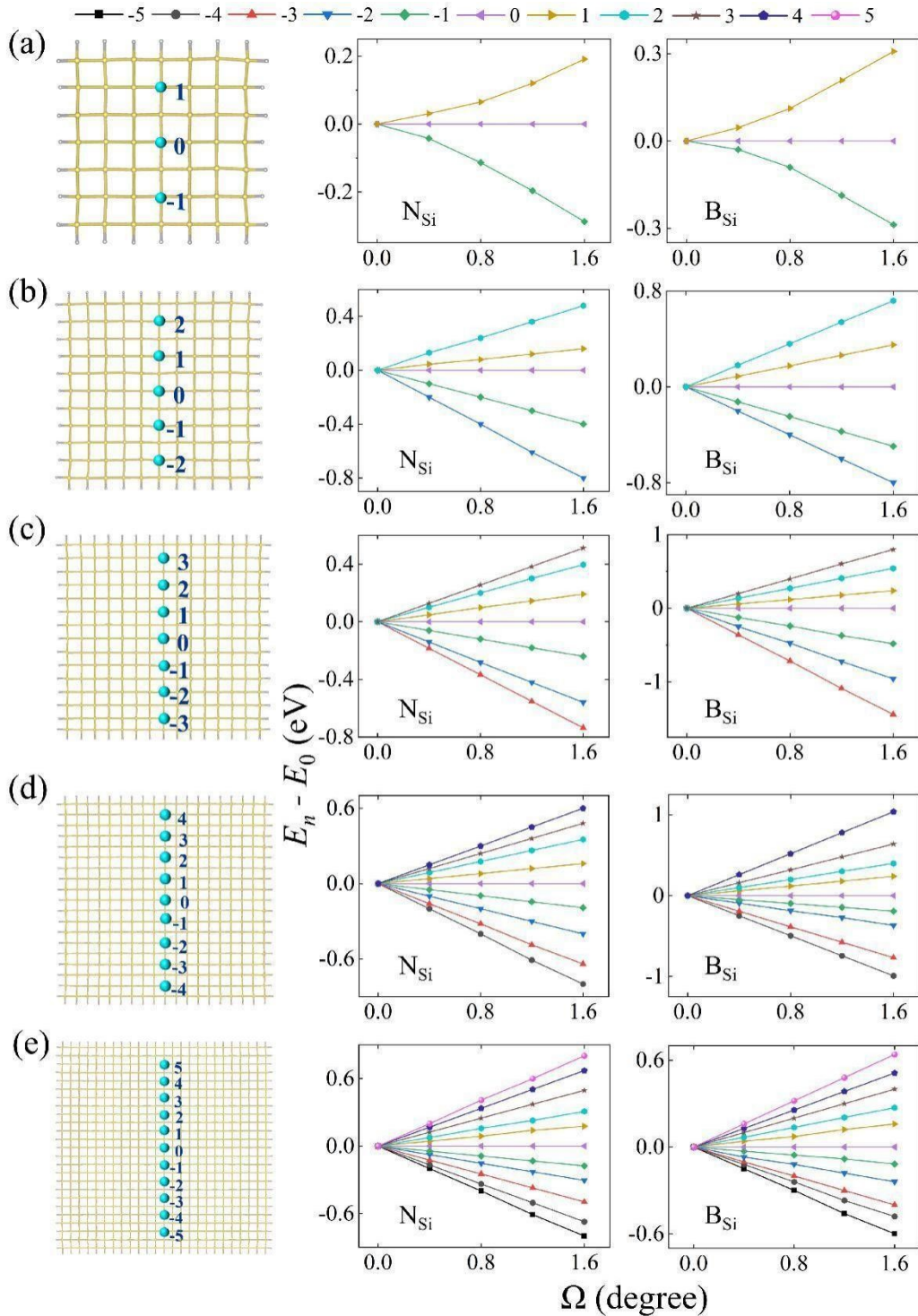


FIG. S19 [001]-oriented SiNW with a diameter of $D =$ (a) 1.15 nm, (b) 1.92 nm, (c) 2.68 nm, (d) 3.45 nm, (e) 4.61 nm, with 11 doping sites (blue balls): sites $n = 1, 2, 3, 4, 5$ are on the

tensile side, sites $n = -1, -2, -3, -4, -5$ are on the compressive side, and site $n = 0$ is on the neutral surface. The last two columns are The relative formation energy $E_n - E_0$ at site n versus bending angle Ω for various doping cases, denoted as X_{Si} ($X = \text{B}, \text{N}$), where the host Si atom is substituted with the dopant X atom.

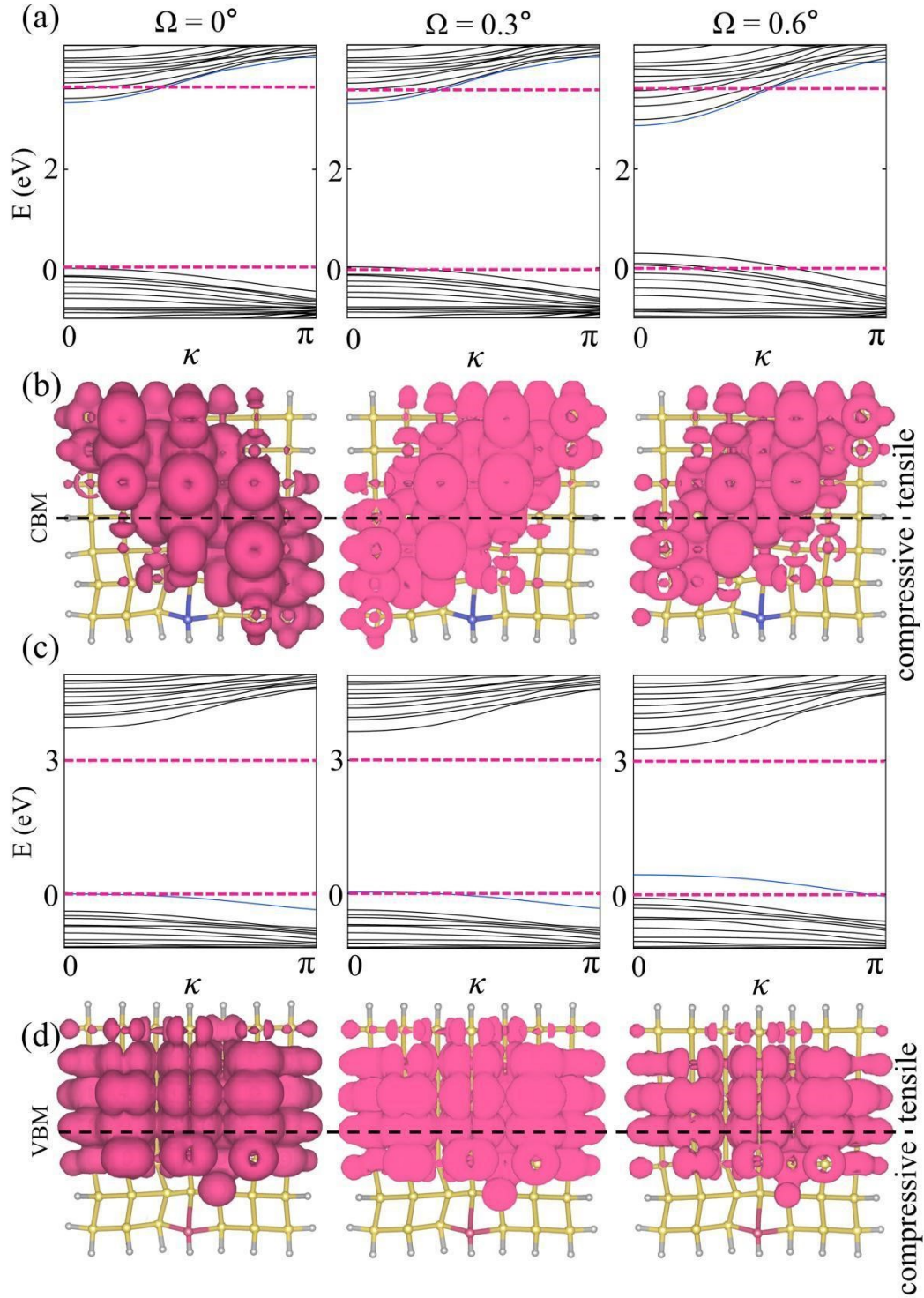


FIG. S20 [001]-oriented SiNW with a diameter of $D = 1.15$ nm after (a) (b) N and (c) (d) B doped at position $n = -4$. (a) (c) Electronic energy bands for strain-free NW and bending angles with $\Omega = 0.3^\circ$ and $\Omega = 0.6^\circ$. Electronic density distribution (pink spheres) for the (b) CBM state and (d) the VBM state. The isosurface level is $1.72 \times 10^{-6} e \text{ \AA}^{-3}$.

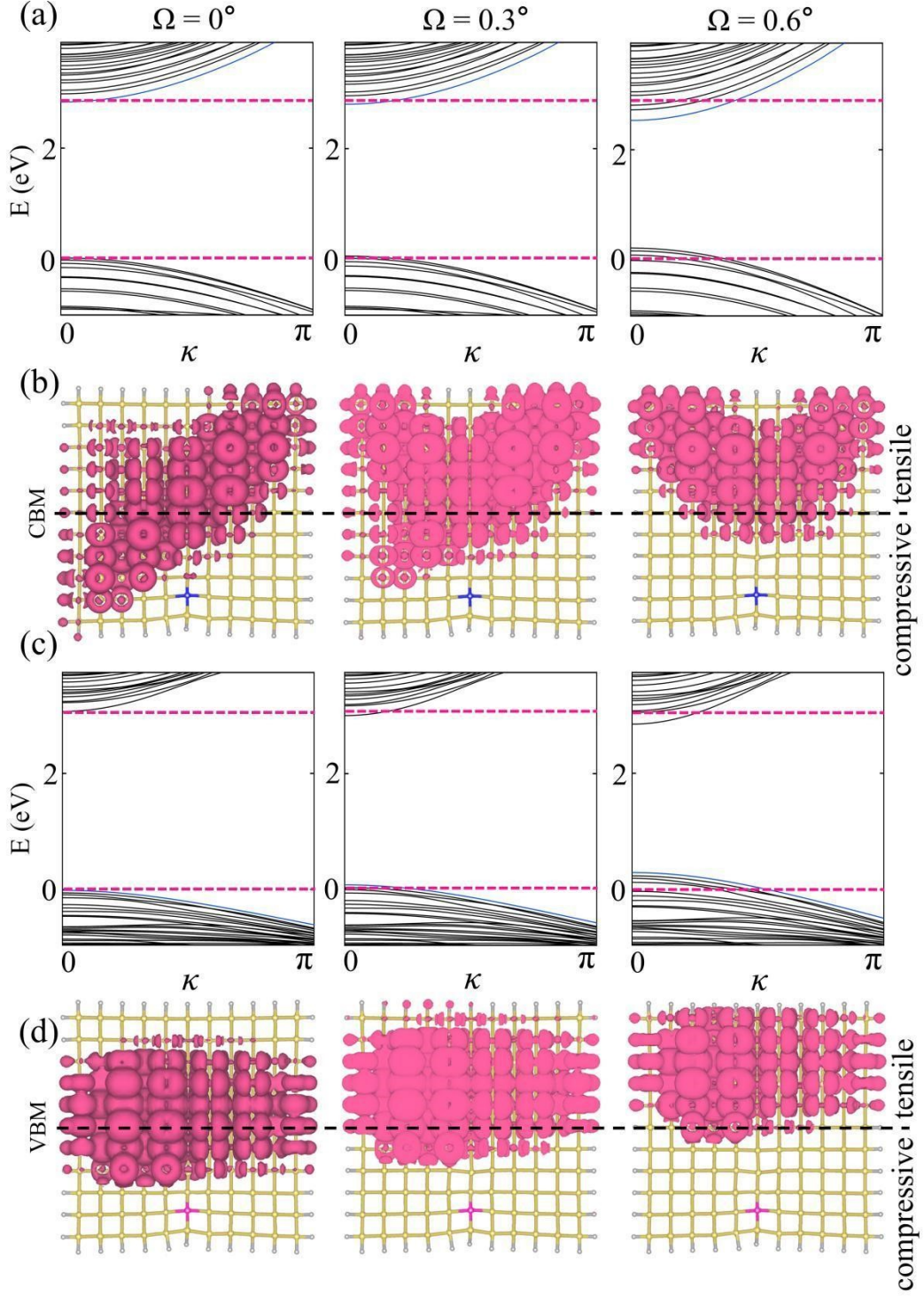


FIG. S21 [001]-oriented SiNW with a diameter of $D = 1.92$ nm after (a) (b) N and (c) (d) B doped at position $n = -4$. (a) (c) Electronic energy bands for strain-free NW and bending angles with $\Omega = 0.3^\circ$ and $\Omega = 0.6^\circ$. Electronic density distribution (pink spheres) for the (b) CBM state and (d) the VBM state. The isosurface level is $1.72 \times 10^{-6} e \text{ \AA}^{-3}$.

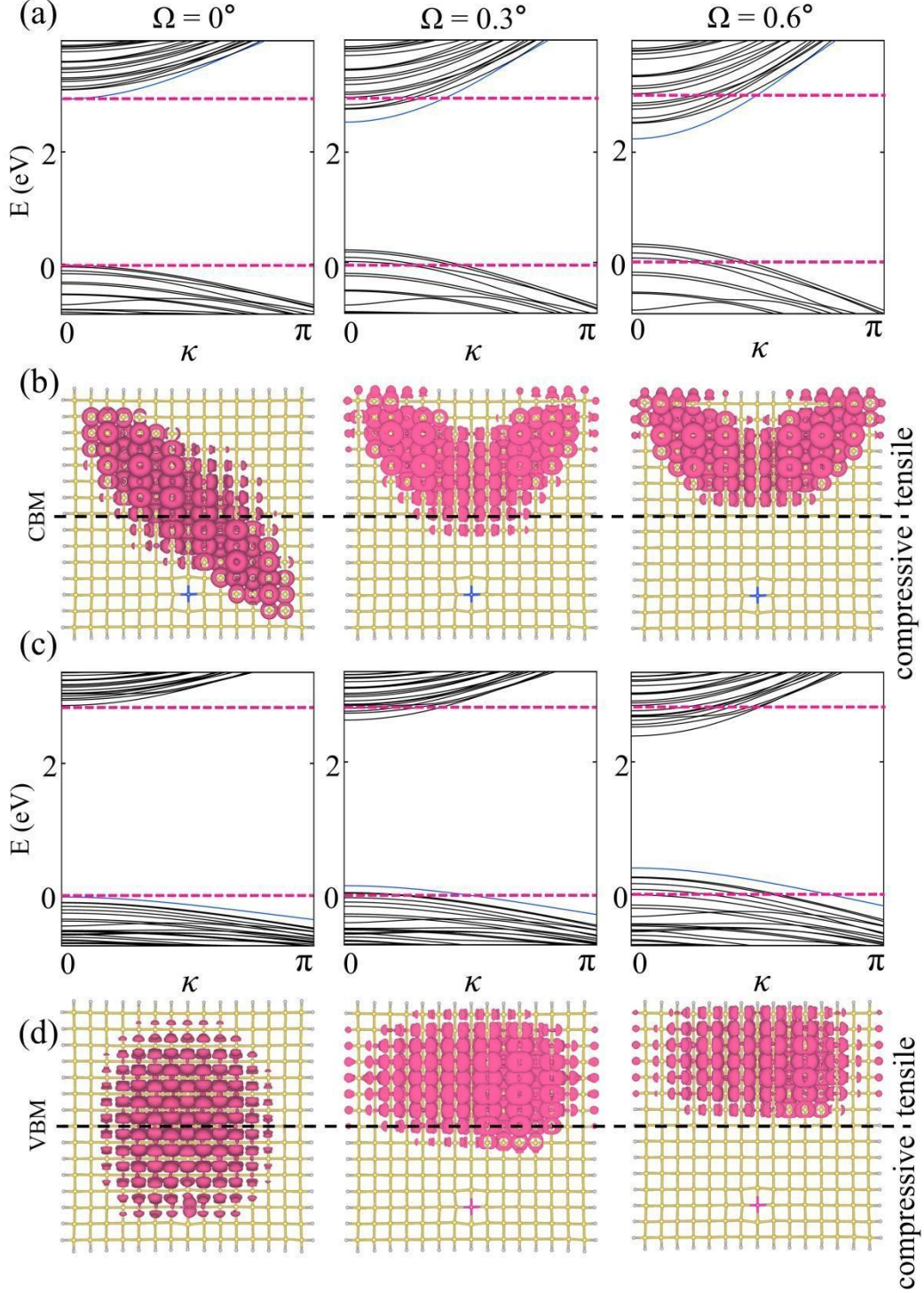


FIG. S22 [001]-oriented SiNW with a diameter of $D = 2.68$ nm after (a) (b) N and (c) (d) B doped at position $n = -4$. (a) (c) Electronic energy bands for strain-free NW and bending angles with $\Omega = 0.3^\circ$ and $\Omega = 0.6^\circ$. Electronic density distribution (pink spheres) for the (b) CBM state and (d) the VBM state. The isosurface level is $1.72 \times 10^{-6} e \text{ \AA}^{-3}$.

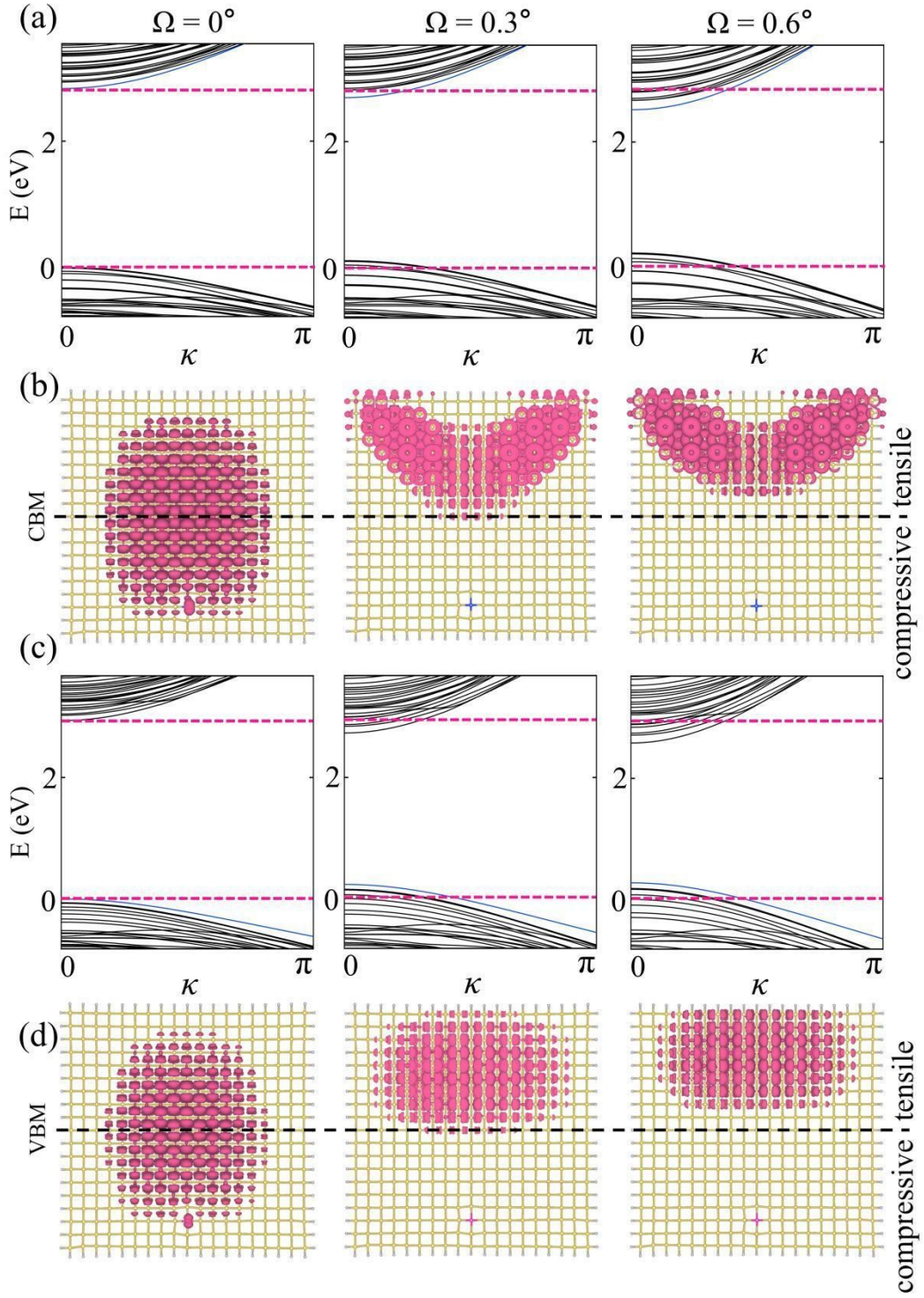


FIG. S23 [001]-oriented SiNW with a diameter of $D = 3.45$ nm after (a) (b) N and (c) (d) B doped at position $n = -4$. (a) (c) Electronic energy bands for strain-free NW and bending angles with $\Omega = 0.3^\circ$ and $\Omega = 0.6^\circ$. Electronic density distribution (pink spheres) for the (b) CBM state and (d) the VBM state. The isosurface level is $1.72 \times 10^{-6} e \text{ \AA}^{-3}$.

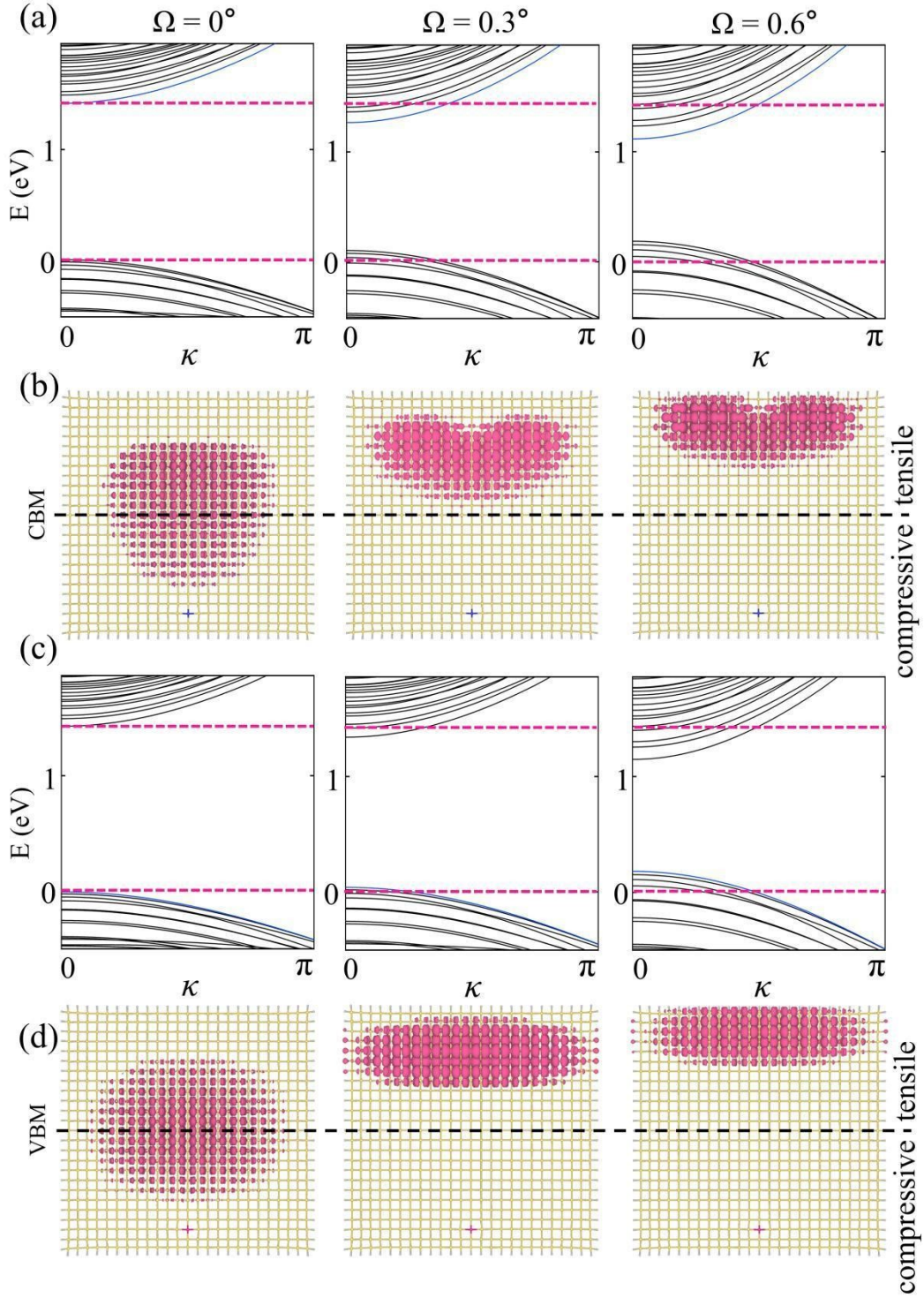


FIG. S24 [001]-oriented SiNW with a diameter of $D = 4.61$ nm after (a) (b) N and (c) (d) B doped at position $n = -4$. (a) (c) Electronic energy bands for strain-free NW and bending angles with $\Omega = 0.3^\circ$ and $\Omega = 0.6^\circ$. Electronic density distribution (pink spheres) for the (b) CBM state and (d) the VBM state. The isosurface level is $1.72 \times 10^{-6} \text{ e \AA}^{-3}$.